AGU PUBLICATIONS

Geophysical Research Letters

RESEARCH LETTER
10.1002/2016GL069372

Key Points:
- The performance of the NEEWS in Taiwan during the 2016 Meinong earthquake which caused 117 deaths is illustrated
- The alarms were issued correctly without any false or missed alarms under a predesignated PGA threshold during the 2016 Meinong earthquake
- The earthquake source effect and site effect were observed in the diagram of the difference between the predicted PGA and the measured PGA

Supporting Information:
- Supporting Information S1

Correspondence to:
T.-Y. Hsu,
tyhsu@mail.ntust.edu.tw

Citation:
Hsu, T.-Y., H.-H. Wang, P.-Y. Lin, C.-M. Lin, C.-H. Kuo, and K.-L. Wen (2016), Performance of the NCREE's on-site warning system during the 5 February 2016 M_w 6.53 Meinong earthquake, *Geophys. Res. Lett.*, *43*, 8954–8959, doi:10.1002/2016GL069372.

Received 29 APR 2016
Accepted 2 AUG 2016
Accepted article online 8 AUG 2016
Published online 5 SEP 2016

Performance of the NCREE's on-site warning system during the 5 February 2016 M_w 6.53 Meinong earthquake

Ting-Yu Hsu[1,2], Hsui-Hsien Wang[2], Pei-Yang Lin[2], Che-Min Lin[2], Chun-Hsiang Kuo[2], and Kuo-Liang Wen[3]

[1]Department of Civil and Construction Engineering, National Taiwan University of Science and Technology, Taipei, Taiwan, [2]National Center for Research on Earthquake Engineering, Taipei, Taiwan, [3]Department of Earth Sciences, National Central University, Taiwan

Abstract The National Center for Research on Earthquake Engineering in Taiwan has developed an on-site earthquake early warning system (NEEWS). The Meinong earthquake with a moment magnitude of 6.53 and a focal depth of 14.6 km occurred on 5 February 2016 in southern Taiwan. It caused 117 deaths, injured 551, caused the collapse of six buildings, and serious damage to 247 buildings. During the Meinong earthquake, the system performance of 16 NEEWS stations was recorded. Based on a preassigned peak ground acceleration (PGA) threshold to issue alarms at different stations, no false alarms or missed alarms were issued during the earthquake. About 4 s to 33 s of lead time were provided by the NEEWS depending on the epicenter distance. In addition, the directivity of the earthquake source characteristic and also possibly the site effects were observed in the diagram of the distribution of PGA difference between the predicted PGA and the measured PGA.

1. Introduction

Since Taiwan suffers from a high potential for seismic hazards from in-land earthquakes, the lead time before a destructive earthquake wave arrives given by a regional earthquake early warning (EEW) system can be null. Therefore, in addition to many existing on-site EEW algorithms [*Nakamura*, 1998; *Odaka et al.*, 2003; *Kanamori*, 2005; *Allen et al.*, 2009; *Böse et al.*, 2012], the National Center for Research on Earthquake Engineering (NCREE) in Taiwan has been developing an on-site EEW system since 2009 to provide more lead time at regions with more potential for damage, i.e., the region close to an epicenter. However, few on-site EEW systems have reported the real-time performance during a damaging earthquake. This paper illustrates how the NCREE's on-site earthquake early warning system (NEEWS) performs during the Meinong earthquake with a moment magnitude of 6.53.

The NEEWS predicts the peak ground acceleration (PGA) of the oncoming earthquake at the same station based on a recently developed support vector machine (SVM) technique [*Hsu et al.*, 2013]. First, six *P* wave features are extracted from the first 3 s of the vertical component of ground motion after *P* wave arrival. These features are predominant frequency, peak ground acceleration, peak ground velocity, peak ground displacement, cumulative absolute velocity, and integration of the squared velocity. The SVM approach is then employed to establish a regression model to predict the PGA according to these *P* wave features. Half of the strong ground motion records of 71 earthquake events records between 1992 and 2006 in the Taiwan Strong Motion Instrumentation Program with local magnitude, M_L, between 3.0 and 7.3 are used to train the regression model. After the regression model is constructed, it is embedded into a MicroBox real-time computation platform with an EpiSensor seismometer [*Lin et al.*, 2012]. The short-term average/long-term average algorithm was applied to automatically determine the *P* wave arrival time in the NEEWS. The *P* wave features and the estimated PGA will be calculated online in the system within 3 s after the system is triggered for 3 s or longer. The technique will issue an alarm if the predicted intensity is higher than a preassigned threshold. Once a warning is issued properly and in a timely fashion, losses due to an earthquake could be greatly mitigated if suitable emergency actions are executed [*Goltz*, 2002]. The NEEWS will activate the broadcast system in schools if an alarm is issued. These schools practice emergency drills annually according to a customized evacuation plan in order to benefit users.

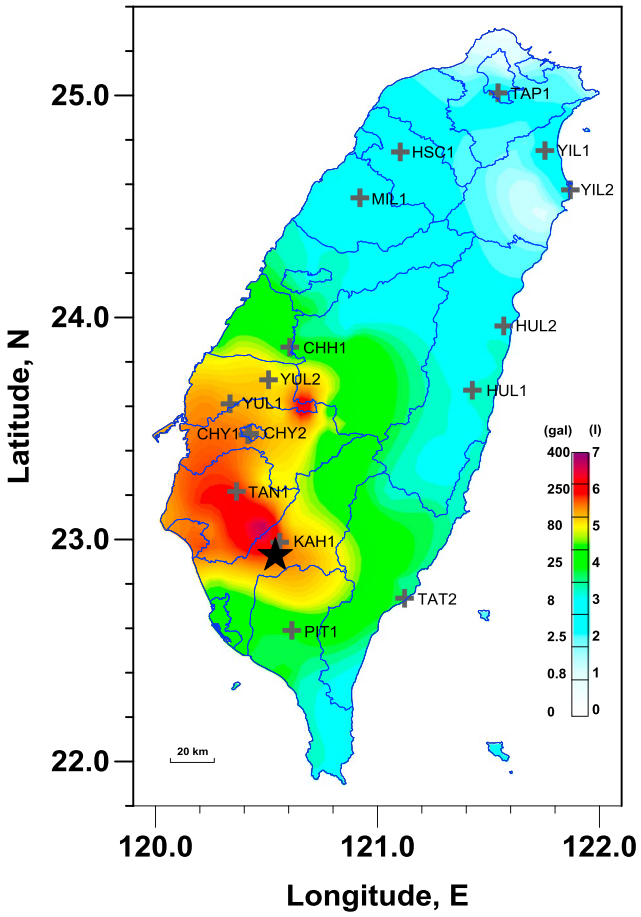

Figure 1. The location of the 16 NEEWS stations. The background is the distribution of the observed values of PGA at all the CWB-RTD stations, the NRTS stations, and the NEEWS stations.

Because the NEEWS could be triggered by many nonearthquake events, currently, the NEEWS solves this particular problem by using two sensors installed at different locations of the same station to conduct a double check procedure before an alarm is launched. The onsite NEEWS composes of a main sensor embedded at 2 m underground to prevent interference from the ground surface and a subsensor either mounted on the top of a building or embedded at about 40 m underground. As a result, the main sensor may be triggered due to a nonearthquake event, but the system would launch the alarm only if the subsensor is also triggered.

2. Data of the Meinong Earthquake

The Meinong earthquake ($M_w = 6.53$) occurred at 03:57 A.M., 6 February 2016, local time (7:57 P.M., 5 February 2016, UTC) and was located at 22.92°N latitude, 120.54°E longitude, and a focal depth of 14.6 km. The earthquake caused 117 deaths, injured 551 people, triggered the collapse of six buildings, and caused serious damage to 247 buildings. During the Meinong earthquake, a total of 80, 30, and 16 valid acceleration time histories were recorded at the Central Weather Bureau (CWB) real-time digital (RTD) stations, NCREE's real-time seismic (NRTS) stations, and NCREE's on-site earthquake early warning system (NEEWS), respectively. The largest measured peak ground acceleration (PGA) was 407.89 Gal and was observed at NRTS's A730 station located north of the epicenter with an epicenter distance of approximately 15 km; meanwhile, a PGA of 401.09 Gal was observed at RTD's CHN3 station located northwest from the epicenter with an epicenter distance of approximately 25 km. However, the PGA measured at NEEWS's KAH1 station with an epicenter distance of 7 km was only 213.3 Gal. Based on the focal mechanism solutions calculated by the CWB and the U.S. Geological Survey, the source rupture plane of the main shock is understood to be an east-west striking (299°) fault dipping 42° toward the north with a left-lateral strike slip where the offset is predominately horizontal and parallel to the fault trace. The distribution of the observed values of PGA at all the CWB-RTD stations, the NRTS stations, and the NEEWS stations is shown in Figure 1. The locations of the 16 NEEWS stations are also plotted in the same figure. It is evident that the region with PGAs higher than 80 Gal extends from the epicenter to its northwest. The strong ground motion distribution may result from the northwestward rupture of the left-lateral strike-slip fault. Additionally, the spread of near-surface soft alluvium around this region may induce site amplification of ground motion to partially cause a distribution of PGA.

3. Performance and Discussion

Based on the experience of seismic reconnaissance in Taiwan, a region with a seismic intensity level of 5 (Shindo scale, as shown in Table 1) or greater, i.e., PGA $>$ 80 Gal, could suffer structural damage, while a region with a seismic intensity level of 4 or greater, i.e., PGA $>$ 25 Gal, could suffer minor damage such as from falling things. Another concern is that due to higher seismic hazard in eastern Taiwan (Yilan County, Hualien County,

Table 1. The Performance Summary of the 16 NEEWS Stations During the Meinong Earthquake

Station Name	Epicenter Distance (km)	Lead Time (s)	Measured PGA (Gal)	Predicted PGA (Gal)	Measured Intensity	Predicted Intensity	Alarm Threshold	Alarm Status
KAH1	7	3.8	213.3	240.3	5	5	4	CA
TAN1	36	8.4	242.0	207.4	5	5	4	CA
PIT1	38	6.9	26.2	49.6	4	4	4	CA
CHY1	60	10.4	184.3	167.7	5	5	4	CA
CHY2	62	10.4	175.8	81.8	5	5	4	CA
TAT2	64	5.4	22.0	70.7	3	4	5	CNA
YUL1	77	12.6	144.2	70.8	5	4	4	CA
YUL2	85	12.8	130.8	41.3	5	4	4	CA
CHH1	104	17.0	49.4	40.2	4	4	4	CA
HUL1	122	20.0	12.8	27.9	3	4	5	CNA
HUL2	155	23.1	9.7	6.9	3	2	5	CNA
MIL1	183	23.5	8.8	1.0	3	1	4	CNA
HSC1	208	32.8	7.1	1.0	2	1	4	CNA
YIL2	226	29.0	6.1	1.0	2	1	5	CNA
YIL1	235	19.9	9.3	4.8	3	2	5	CNA
TAP1	252	4.7	6.3	17.4	2	3	4	CNA

and Taitung County), the seismic design code in Taiwan requests a higher level of design ground excitation in eastern Taiwan. Since the seismic capacity of the structures and nonstructures in eastern Taiwan is higher, the earthquake intensity likely to induce damage in that region is also higher. Therefore, the threshold of the stations in eastern Taiwan is set as intensity 5, while the threshold of the other stations is set to intensity 4. During the Meinong earthquake, the signal to broadcast an alarm was sent to the controller immediately at the NEEWS's stations if the predicted seismic intensity was larger or equal to the preassigned threshold. However, the sound was muted by the controller since the earthquake occurred before dawn, and the schools were empty of people. If the signal to broadcast was sent to the controller during the school time, then the alarm would be announced by the broadcast system.

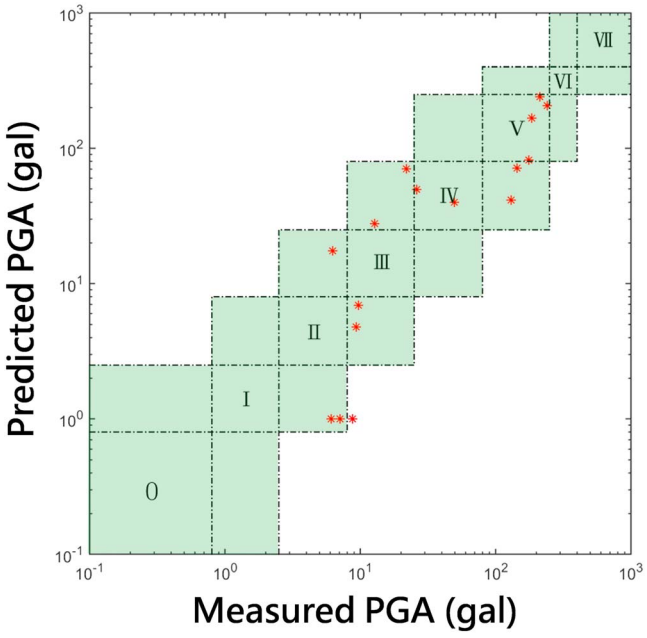

Figure 2. The distribution of measured PGA and predicted PGA for the 16 NEEWS stations. The predicted PGA corresponds to the measured PGA very well in a logarithm scale. The standard deviation of the difference between the predicted PGA and the measured PGA is about 40.8 Gal. The intensity difference for all stations is within the range of plus one or minus one level (the region with a green background), except the one at the MIL1 station. The measured PGA at the MIL1 station was 8.8 Gal, which is just above the threshold of the third seismic intensity level, i.e., 8.0 Gal, while the predicted seismic intensity was level 1.

First, the accuracy of the predicted PGA during the Meinong earthquake is considered. The comparison of the predicted PGA and the measured PGA of all the 16 stations is plotted in Figure 2. It can be observed that the predicted PGA corresponds to the measured PGA very well in a logarithm scale. The standard deviation of the difference between the predicted PGA and the measured PGA is approximately 40.8 Gal. As for the difference in the seismic intensity that is used as the basis to issue an alarm for general applications, as shown in the same figure, the intensity difference for all stations is within the range of plus one or minus one level, except the one at the MIL1 station. The measured PGA at the MIL1 station was 8.8 Gal, which is just above the

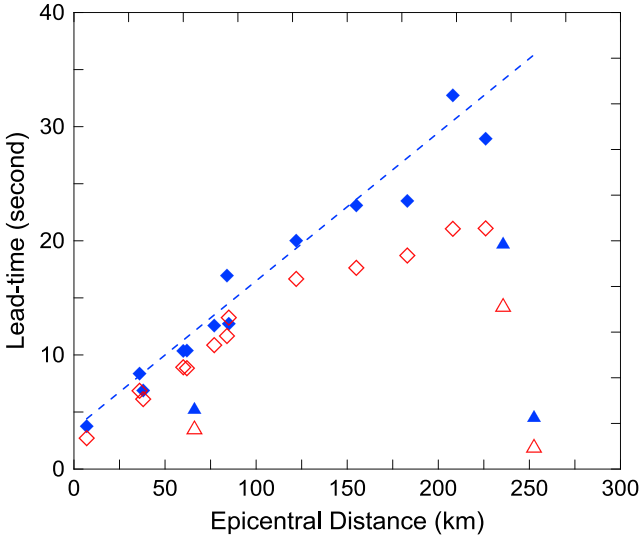

Figure 3. The correlation between the lead time and the epicenter distance at the NEEWS stations. The blue solid diamonds and triangles represent the lead time before PGA arrival, while the dashed blue line represents the general trend of most of the stations as marked using blue solid diamonds. The lead times before *S* wave arrival are also plotted as the red hollow diamonds and triangles for reference. The triangles represent the TAT2 station, YIL1 station, and TAP1 station in increasing epicenter distance from small to large, and these three stations behave quite differently compared to the trend of the other stations.

threshold of the third seismic intensity level, i.e., 8.0 Gal, while the predicted seismic intensity was level 1. However, since the measured seismic intensity was smaller than the threshold to issue an alarm, this underestimated intensity case affected nothing in practice. In summary, the rate of accurate predicted intensity was 93.75%.

As for the accuracy of issued alarms, four conditions are defined as follows: (1) correct alarm (CA), when both the measured intensity and the predicted intensity reach the alarm threshold; (2) correct no alarm (CNA), when both the measured intensity and the predicted intensity are smaller than the alarm threshold; (3) missed alarm (MA), when the measured intensity reaches the alarm threshold but the predicted intensity is smaller than the alarm threshold; and (4) false alarm (FA), when the measured intensity is smaller than the alarm threshold but the predicted intensity reaches the alarm threshold. During the Meinong earthquake, according to the preassigned threshold at each station, eight stations were classified as CA, and eight stations were classified as CNA. In other words, the alarm conditions of all the 16 stations were correct (see Table 1). The rate of successful alarms was 100%.

Meanwhile, the lead time gained by the NEEWS is defined as the time interval between the time an alarm is issued and the time of the PGA arrival. In the Meinong earthquake, by observing the relationship between the lead time and the epicenter distance in Figure 3 and Table 1, it is evident that the lead time generally increases with the epicenter distance, and the trend of most stations (blue solid diamonds in Figure 3) is illustrated as a dashed blue line in the same figure. At the KAH1 station with only a 7 km epicenter distance, the lead time was about 3.8 s (Figure S1 in the supporting information). At the TAN1 station, which is close to the region suffering serious damage (with about 36 km epicenter distance), the lead time was about 8.4 s (supporting information Figure S2). The other regions with a seismic intensity level of 5 also received about 10 ~ 13 s of lead time (e.g., CHY1 station in the supporting information Figure S3). In addition, in Figure 3, there are three stations (blue solid triangles) with quite different trends from the trends of the other stations. Theoretically, the farthest station should receive the longest lead time. However, the TAP1 station with the longest epicenter distance only receives 4.7 s of lead time. This is probably due to a poor signal-to-noise ratio (SNR). The *P* wave seems to have been too small to trigger the system until the arrival of the *S* wave with a larger amplitude (supporting information Figure S4). A similar phenomenon can be observed at the YIL1 station whose epicenter distance was about 235 km, which is not shown in this paper. Fortunately, since the seismic intensity of the stations with a low SNR is usually not large enough to issue an alarm, practically, no negative consequence will be induced. Furthermore, the lead time at the TAT2 station is also much smaller than the trend. Observation of the measured acceleration time history in the supporting information Figure S5 shows that the PGA occurred at the vertical component rather than at the horizontal components. This phenomenon is not observed in all the other stations probably due to source directivity, which will be shortly discussed. Another possible reason could be the site condition, but since this station was established in December 2015, there is insufficient earthquake data to interpret the site effect at this new station. In Figure 3, the lead time before *S* wave arrival of each station is also plotted as the red hollow diamonds and triangles. It is observed that comparing to the lead time before PGA arrival, the lead time before *S* wave

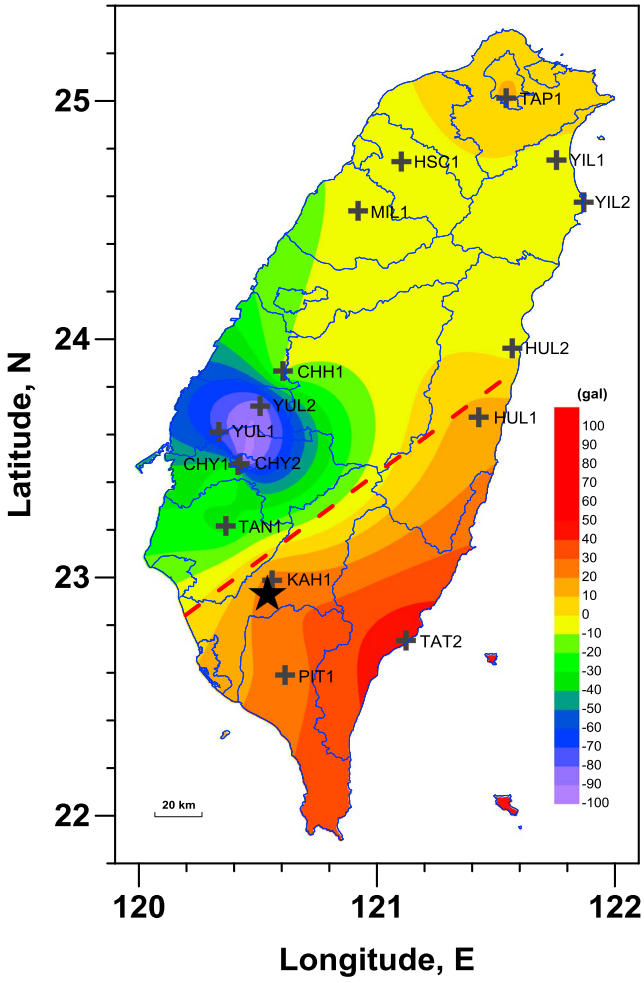

Figure 4. The distribution of the PGA difference. The PGA difference is defined as the predicted PGA minus the measured PGA. All the PGA differences of the region in the southeastern portion divided by the red line is positive. On the other hand, all the PGA differences of the region in the northwestern portion is negative, except the TAP1 station located in the Taipei basin.

arrival of the stations within the region with a seismic intensity level of 5 only reduce about 1 s. The lead time of the other stations outside the region with a seismic intensity level of 5 are reduced more, about 3 s to 12 s.

The PGA difference is defined as the predicted PGA minus the measured PGA ($PGA_{diff} = PGA_{pred}$-PGA_{meas}). The distribution of the PGA difference is shown in Figure 4. It can be observed that all the PGA differences of the region in the southeastern portion divided by the red line close to the epicenter in the same figure is positive. On the other hand, all the PGA differences of the region in the northwestern portion are negative, except for the TAP1 station located in the Taipei basin. The mean and standard deviation of the PGA differences for the stations at the region in the southeastern portion and in the northwestern portion in Figure 4 are calculated, respectively, but only the stations with epicenter distance less than 100 km since the source directivity should mainly affect the stations close to the epicenter. The mean and standard deviation of the PGA differences of the KAH1, PIT1, and TAT2 stations in the southeastern portion is 33.0 Gal and 13.7 Gal, while the ones of the TAN1, CHY1, CHY2, YUL1, and YUL2 stations in the northwestern portion is −61.6 Gal and 34.4 Gal. This phenomenon possibly implies the existence of directivity of the earthquake source rupture. In other words, the reason that most of the predicted PGA at the stations in the northwestern portion is lower than the measured PGA could be the accumulation of a seismic wave due to fault rupture from the epicenter in the northwest direction. On the contrary, for the stations in the southeast portion, the seismic amplitude could be dispersed if the fault ruptures along an opposite direction from these stations. Note that the effect of source direction is not considered in the current embedded SVM algorithm. Similarly, the site effect could also be observed in the same figure since the current embedded SVM algorithm does not accommodate it either. For instance, the predicted PGA at the region around the YUL1 station, YUL2 station, and CHY2 station is much more underestimated than the other stations, probably due to site effects. As for the TAP1 station where the predicted PGA is higher than the measured PGA, the reason could be estimation of the predicted PGA being based on the unexpected *S* wave rather than the *P* wave due to a low SNR (supporting information Figure S4) as previously mentioned.

Besides the performance of the NEEWS during the Meinong earthquake, the general performance of the NEEWS is also discussed here. Till now, there were 10,443 triggered events without corresponding events in the earthquake catalog using the SVM technique and two-sensor approach. Among them, only two false alarms with predicted intensity level 4 was launched. These false alarms were due to abnormal signals of two newly established stations when the systems were not stable yet in the beginning. On the other hand,

there were 1536 triggered earthquake events with corresponding events in the earthquake catalog. Among them, only one missed alarm with measured PGA 27.83 Gal was observed. The standard deviation of the PGA difference of these earthquake events was 14.19 Gal. In general, the performance of the NEEWS is quite promising.

4. Conclusions and Future Works

The Meinong earthquake that caused the deaths of more than 100 people and serious damage to more than 200 buildings was a good opportunity to validate the performance of the NEEWS systems. The NEEWS issued alarms 3 s immediately after being triggered. The alarms were successfully issued at eight stations without any false alarm. Meanwhile, no alarms were issued at the remaining eight stations without any missed alarm. The lead time obtained ranged from about 4 s to 33 s depending on the distance to the epicenter. Even for a region close to the epicenter with a measured intensity level equal to or greater than 5, about 4 ~ 13 s of lead time was provided by the NEEWS. Although it was observed that a low SNR of the seismic wave measured at the stations with a long epicenter distance could shorten the lead time, this phenomenon, in fact, will induce no practical effects since no alarms should be issued, regardless of how much lead time is provided. Apparently, the on-site EEW systems developed by NCREE have great potential to reduce seismic losses, especially for the regions close to an epicenter where damage is more likely to occur and these regions could be within the blind zone of a regional EEW system.

Interestingly, the distribution of the PGA difference between the predicted PGA and the measured PGA could show the directivity of the earthquake source characteristic and also possibly the site effects. This illustrates that the current prediction model of the NEEWS system has not accommodated these two factors very well. Therefore, there is still a great opportunity for the accuracy of the predicted PGA to be improved in future research.

Since late 2014, the Ministry of Education and the Ministry of Science and Technology in Taiwan have been facilitating the application of the NEEWS in all public elementary and junior high schools in Taiwan. More than 3000 schools are planned to be equipped with the NEEWS in 2017. Hopefully, by combining it with earthquake disaster prevention education and emergency drills, earthquake losses could be greatly reduced by using the EEW techniques in the near future in these schools.

Note that although the NEEWS seems to perform well for most of the experienced earthquakes, the predicted PGA of the earthquakes with source duration time much longer than 3 s could be underestimated, due to the information carried by the first few seconds of *P* wave is limited. This phenomenon is anticipated for either on-site EEWS or regional EEWS and has been experienced during the 2011 Tohoku earthquake in Japan. The estimation of seismic intensity could be greatly improved if longer earthquake records after trigger is used; however, the response time is sacrificed. Future research to overcome the challenge of EEW techniques due to long or complex slip propagation process is still required.

Acknowledgments
This research was supported in part by the Ministry of Science and Technology of the Republic of China under the grant MOST 104-2625-M-492-008. The authors would like to thank the Central Weather Bureau for providing data of the real-time data stations. The data used are in the supporting information.

References

Allen, R. M., P. Gasparini, O. Kamigaichi, and M. Böse (2009), The status of earthquake early warning around the world: An introductory overview, *Seismol. Res. Lett.*, *80*, 682–693, doi:10.1785/gssrl.80.5.682.

Böse, M., T. Heaton, and E. Hauksson (2012), Rapid estimation of earthquake source and ground-motion parameters for earthquake early warning using data from a single three-component broadband or strong-motion sensor, *Bull. Seismol. Soc. Am.*, *102*(2), 738–750.

Goltz, J. (2002), Introducing earthquake early warning in California: A summary of social science and public policy issues A report to OES and the operational areas, Disaster Assistance Div., Caltech Seismol. Lab., Pasadena, Calif.

Hsu, T. Y., S. K. Huang, Y. W. Chang, C. H. Kuo, C. M. Lin, T. M. Chang, K. L. Wen, and C. H. Loh (2013), Rapid on-site peak ground acceleration estimation based on support vector regression and *P*-wave features in Taiwan, Soil Dynam, *Earthquake Eng.*, *49*, 210–217, doi:10.1016/j.soildyn.2013.03.001.

Kanamori, H. (2005), Real-time seismology and earthquake damage mitigation, *Annu. Rev. Earth Planet. Sci.*, *33*, 195–214.

Lin, P. Y., S. K. Huang, H. W. Chiang, and Z. P. Shen (2012), Development of the on-site earthquake early warning system in Taiwan, in *Proc 15th World Conf. on Earthq. Eng*, Lisbon, Portugal.

Nakamura, Y. (1998), *A New Concept for the Earthquake Vulnerability Estimation and Its Application to the Early Warning System*, Proc Early Warning Conf Potsdam, Germany.

Odaka, T., K. Ashiya, S. Tsukada, S. Sato, K. Ohtake, and D. Nozaka (2003), A new method of quickly estimating epicentral distance and magnitude from a single seismic record, *Bull. Seismol. Soc. Am.*, *93*(1), 526–532.